



Published in final edited form as:

*Eur J Pharm Sci.* 2009 May 12; 37(2): 141–150. doi:10.1016/j.ejps.2009.02.008.

## ICAM-1 Targeting of Doxorubicin-Loaded PLGA Nanoparticles to Lung Epithelial Cells

Chittasupho Chuda, Xie Sheng-Xue, Baoum Abdulgader, Yakovleva Tatyana, Siahaan J. Teruna, and Berkland Cory\*

Department of Pharmaceutical Chemistry, School of Pharmacy, The University of Kansas, Lawrence, Kansas, 66047

### Abstract

Interaction of leukocyte function associated antigen-1 (LFA-1) on T-lymphocytes and intercellular adhesion molecule-1 (ICAM-1) on epithelial cells controls leukocyte adhesion, spreading, and extravasation. This process plays an important role in leukocyte recruitment to a specific site of inflammation and has been identified as a biomarker for certain types of carcinomas. Cyclo-(1,12)-PenITDGEATDSGC (cLABEL) has been shown to inhibit LFA-1 and ICAM-1 interaction via binding to ICAM-1. In addition, cLABEL has been shown to internalize after binding ICAM-1. The possibility of using cLABEL conjugated nanoparticles (cLABEL-NP) as a targeted and controlled release drug delivery system has been investigated in this study. The cLABEL peptide was conjugated to a modified Pluronic<sup>®</sup> surfactant on poly (DL-lactic-co-glycolic acid) (PLGA) nanoparticles. The cLABEL-NP showed more rapid cellular uptake by A549 lung epithelial cells compared to nanoparticles without peptide. The specificity of ICAM-1 mediated internalization was confirmed by blocking the uptake of cLABEL-NP to ICAM-1 using free cLABEL peptide to block the binding of cLABEL-NP to ICAM-1 on the cell surface. Cell studies suggested that cLABEL-NPs targeted encapsulated doxorubicin to ICAM-1 expressing cells. Cytotoxicity assay confirmed the activity of the drug incorporated in nanoparticles. Sustained release of doxorubicin afforded by PLGA nanoparticles may enable cLABEL-NP as a targeted, controlled release drug delivery system.

### Keywords

ICAM-1; peptide; PLGA; nanoparticles; targeting

### 1. Introduction

Interaction of leukocyte function associated antigen-1 (LFA-1) and intercellular cell adhesion molecule-1 (ICAM-1) can play a critical role in tumor metastasis and progression [Yusuf-Makagiansar et al., 2002], [Hopkins et al., 2004], [Wojcikiewicz et al., 2003], [McDawa et al., 1998], [Dunehoo et al., 2006] and [Yusuf-Makagiansar et al., 2001]. ICAM-1 is expressed on a variety of inflammatory and immune effector cells as well as endothelial cells, fibroblasts, and epithelial cells [Melis et al., 1996]. ICAM-1 is also up-regulated on the surface of a variety of lymphomas, melanomas, renal, pancreatic, bladder and lung carcinomas and/or their local

\*Address for correspondence: Cory Berkland, Department of Pharmaceutical Chemistry and Chemical and Petroleum Engineering 2095 Constant Ave Lawrence, Kansas 66047 Phone: (785) 864-1455 Fax: (785) 864-1454 berkland@ku.edu.

**Publisher's Disclaimer:** This is a PDF file of an unedited manuscript that has been accepted for publication. As a service to our customers we are providing this early version of the manuscript. The manuscript will undergo copyediting, typesetting, and review of the resulting proof before it is published in its final citable form. Please note that during the production process errors may be discovered which could affect the content, and all legal disclaimers that apply to the journal pertain.

vascular network [Melis et al., 1996]. The expression of ICAM-1 may be involved in the regulation of tumor susceptibility to the activity of defensive cells. The upregulation of ICAM-1 expression on some types of carcinomas such as melanomas and lung carcinomas may be followed by the extracellular release of soluble ICAM-1 (sICAM-1) [Melis et al., 1996]. The sICAM-1 could interfere with the interaction of surface ICAM-1 and immune cells such as natural killer (NK) cells or lymphocyte activated killer (LAK) cells by competition, leading to the reduction of cancer cell exposure to these protective cells [Melis et al., 1996]. Shedding of sICAM-1 in the extracellular space has been proposed as one of the mechanisms that tumor cells use to escape cell-mediated cytotoxicity [Melis et al., 1996].

A cyclic peptide, cyclo-(1,12)-PenITDGEATDSGC (cLABL), derived from the I-domain of the  $\alpha_L$ -subunit of LFA-1 integrin has been shown to impair LFA-1/ICAM-1 interaction by binding to the D<sub>1</sub> domain of ICAM-1. This peptide specifically inhibited homotypic and heterotypic T-cell adhesion to epithelial and endothelial cell monolayers by disrupting the LFA-1/ICAM-1 interaction [Anderson and Siahaan, 2003a], [Anderson et al., 2004], [Anderson and Siahaan, 2003b], [Yusuf-Makagiansar and Siahaan, 2001] and [Yusuf-Makagiansar et al., 2007]. In addition to its receptor binding characteristics, cLABL displayed receptor mediated endocytosis, insinuating a possible use as a targeting moiety for intracellular drug delivery [Yusuf-Makagiansar and Siahaan, 2001]. Accordingly, cLABL conjugated nanoparticles were proposed to be a promising anti-cancer drug delivery system targeting ICAM-1.

Recently, monoclonal antibodies have become crucial therapeutic agents against a wide range of cancers. However, autoimmune reactions and short half-lives are often encumbrances for immunotherapy using monoclonal antibodies [Tibetts et al., 2000], [Wofsy, 1985] and [Huang et al., 2005]. Peptides and small molecule inhibitors may offer similar therapeutic interventions by acting as a targeting ligand to proteins on the cell surface [Yusuf-Makagiansar et al., 2002]. Furthermore, in comparison to monoclonal antibodies, cyclic peptides have been shown to offer improved physicochemical stability and may even improve selectivity to the targeted site [Yusuf-Makagiansar et al., 2002] and [Yusuf-Makagiansar et al., 2001].

The utmost ambition of pharmaceutical therapy is to deliver the drug carriers to a specific therapeutic site of action with a triggered or sustained drug release. Advantages of this modality could include a decrease in adverse effects, lower toxicity, an increase in the efficacy of the therapeutic agent and a reduction in the frequency of administration. Polymeric nanoparticles (NP) possess some advantages over other formulations in terms of stability and feasibility of modulating the drug release profile by controlling polymer degradation [Avgoustakis, 2004] and [Guerrouache et al., 2006]. In addition, this delivery system permits functional group modification on the nanoparticle surface without compromising the activity of the drug carried.

In this study, cLABL-conjugated poly (DL-lactic-co-glycolic acid) nanoparticles (cLABL-NP) targeting ICAM-1 on A549 lung epithelial cells have been formulated and characterized. Binding and internalization studies have demonstrated that nanoparticles can be targeted to these epithelial cells via ICAM-1 and can be internalized into the cells rapidly. The cellular internalization was confirmed by utilizing fluorescence markers and microscopy. Interestingly, the results indicated that cLABL-NP trafficked to lysosomes and escaped lysosomal sequestration. Targeting and drug release studies of nanoparticles encapsulating doxorubicin (DOX-NP) suggested that PLGA nanoparticles targeted by cLABL localized this drug within A549 cells to offer sustained release. The IC<sub>50</sub> of nanoparticles encapsulating doxorubicin, both conjugated and not conjugated with peptide compared to that of free doxorubicin HCl were reported. Ultimately, cLABL-nanoparticles may be aerosolized to provide a targeted anti-cancer drug delivery system directly to the pulmonary epithelium.

## 2. Materials and Methods

### 2.1 Materials

Poly(DL-lactic-co-glycolic acid) (50:50) with terminal carboxylate group (PLGA, inherent viscosity 0.22 dL/g, Mw ~ 20 kDa and 0.67 dL/g, Mw ~ 90 kDa) was purchased from LACTEL Absorbable Polymers International (Pelham, AL, USA). Pluronic®F-127, Texas Red Dextran (10,000 Mw, lysine fixable) and 4',6-diamidino-2-phenylindole, dilactate (DAPI, dilactate) were purchased from Invitrogen Molecular Probes, Inc. (Carlsbad, CA, USA). 1-Ethyl-3-[3-dimethylaminopropyl]carbodiimide hydrochloride (EDC) and *N*-hydroxysulfosuccinimide (sulfo-NHS) were purchased from Thermo Fisher Scientific Inc. (Rockford, IL, USA). Coumarin-6 was obtained from Polysciences, Inc. (Warrington, PA, USA). Doxorubicin HCl for injection was provided by Novaplus (Irving, TX, USA). Dialysis membrane (MWCO 100,000) was purchased from Spectrum laboratory Products Inc. (Rancho Dominguez, CA, USA). F-12K medium and A549 cell line were obtained from American Type Culture Collection (Manassas, VA, USA). Recombinant, Human, Tumor Necrosis Factor- $\alpha$  (TNF- $\alpha$ ) was purchased from Promega (Madison, WI, USA). Human Interferon gamma was purchased from Roche Diagnostics Corporation (Indianapolis, IN, USA), 3,3',5,5'-Tetramethylbenzidine (TMB) was obtained from Sigma (St. Louis, MO, USA). Monoclonal anti-human CD54 (ICAM-1) Domain D1 was purchased from Ansell (Bayport, MN, USA) and Horseradish Peroxidase-Conjugated Goat Anti-Mouse IgG was obtained from Cayman Chemical (Ann Arbor, MI, USA). CellTiter 96® AQueous Non-Radioactive Cell Proliferation Assay (MTS) was purchased from Promega (Madison, WI, USA)

### 2.2 Methods

**Pluronic®F-127 functional group modification**—Terminal hydroxyl groups on Pluronic®F-127 were converted to carboxyl groups according to the following procedure [Guerrouache et al., 2006]. Pluronic®F-127 (2 g) was dissolved in tetrahydrofuran (THF, 60 ml). Then 4-dimethylaminopyridine (DMAP, 98 mg), triethylamine (108  $\mu$ l) and succinic anhydride (800 mg) were added. The mixture was stirred for 48 hr at room temperature. The solution was dried by rotary evaporation, and, was then dissolved in carbon tetrachloride (30 ml). The excess succinic anhydride was removed by filtration. The Pluronic®F-127-COOH was purified by precipitation with ice-cold diethylether. The product was identified by <sup>1</sup>H NMR spectroscopy (Bruker AVANCE 400 MHz spectrometer) and FTIR spectroscopy (ABB Bomem MB series).

**Preparation of PLGA nanoparticles encapsulating coumarin-6**—Nanoparticles encapsulating a fluorescence marker, coumarin-6, were formulated using a solvent displacement method [Avgoustakis, 2004]. In brief, PLGA, inherent viscosity 0.22 dl/g or 0.67 dl/g) was dissolved in trifluoroethanol (TFE, 18 mg/ml) containing coumarin-6 (95  $\mu$ g). The solution was slowly transferred to a water phase containing surfactant; 0.1% Pluronic®F-127-COOH (35 ml) under mild stirring (250 RPM). The nanoparticles were spontaneously formed due to the rapid removal of TFE. Excess surfactant was removed by dialysis against a 0.2% mannitol solution for 48 hr.

**Preparation of PLGA nanoparticles encapsulating doxorubicin**—Doxorubicin HCl for injection (2 mg/ml) was lyophilized and neutralized using triethylamine (108  $\mu$ mol). The non-aqueous form of doxorubicin was extracted using methylene chloride and evaporated [Kim et al., 2008]. In brief, PLGA (0.22 dl/g or 0.67 dl/g) in acetone solution (18 mg/ml) was mixed with 1.8 mg of the purified doxorubicin. The solution was infused (17.5 ml/hr) into 10 ml of 0.1% Pluronic®F-127-COOH (250 rpm) to allow the formation of nanoparticles encapsulating doxorubicin (DOX-NP). Nanoparticles were collected by centrifugation (15,000 rpm, 40 min) and washed three times. The nanoparticles encapsulating doxorubicin conjugated

with cLABL (cLABL-DOX-NP) was prepared using the method described above. The encapsulation efficiency was determined by centrifugation (13,000 rpm, 40 min) of the DOX-NP or cLABL-DOX-NP suspension (200  $\mu$ l) by collecting the pellet and dissolving in DMSO (200  $\mu$ l). Doxorubicin content was analyzed by fluorescence spectroscopy (Spectramax M5, ex: 500 nm, em: 600 nm).

**Conjugation of cLABL peptide to PLGA-nanoparticles**—A Pluronic<sup>®</sup>F-127-COOH coated PLGA nanoparticles (1.5 mg/ml) suspension was buffered using 2-(*N*-morpholino) ethanesulfonic acid (MES) pH 6.5. Nanoparticles were then incubated with 100 mM 1-Ethyl-3-[3-dimethylaminopropyl]carbodiimide hydrochloride (EDC) and 50 mM *N*-hydroxysulfosuccinimide (sulfo-NHS) for 15 min [Cheng et al., 2007]. The activated carboxyl terminus of Pluronic<sup>®</sup> F127-COOH on the surface of nanoparticles was allowed to react with the amino terminus of the cLABL peptide (80  $\mu$ M) at least 6 hr at room temperature. Conjugated NP were collected by centrifugation (10,000 rpm, 10 min) and washed three times with purified water. Size and charge of NP and cLABL-NP were characterized using dynamic light scattering (ZetaPALS, Brookhaven instrument Inc.). The amount of free cLABL after the reaction was quantified by gradient reversed phase HPLC (SHIMADZU) using a C<sub>18</sub> column. The HPLC consisted of SCL-10A SHIMADZU system controller, LC-10AT VP SHIMADZU liquid chromatograph, SIL-10A XL SHIMADZU autoinjector set at 10  $\mu$ l injection volume, DGU-14A SHIMADZU degasser, sample cooler, and SPD-10A SHIMADZU UV-Vis detector (220 nm). The HPLC-UV system was controlled by a personal computer equipped with SHIMADZU class VP Software. All separations were carried out using a Vydac<sup>®</sup> HPLC column Protein and Peptide C<sub>18</sub> column. Gradient elution was carried out at constant flow of 1 ml/min, from 100% A to 0% A (corresponding to 0% B to 100% B) for 15 min, followed by an isocratic elution at 100% B for 3 min. Mobile phase compositions were (A) acetonitrile-water (5:95) with 0.1% TFA (B) acetonitrile-water (90:10, v/v) with 0.1% trifluoroacetic acid (TFA). At the end of each analysis, the cartridge was re-equilibrated at 1 ml/min flow rate for 13 min with A. The density of peptide on the surface of nanoparticles was calculated from the total surface area assuming a normal Gaussian particle size distribution.

**Drug release study of nanoparticles encapsulating doxorubicin**—The release of doxorubicin from cLABL-DOX-NP or DOX-NP was investigated using 0.1M acetate buffer pH 4 and phosphate buffer pH 7.4 as dissolution media. One milliliter of DOX-NP (4 mg/ml) or five hundred microliters of cLABL-DOX-NP (4 mg/ml) were placed in the dialysis membrane (MwCO 10,000) immersed in 100 ml and 50 ml of buffer solution, respectively and were shaken at 100 rpm, 37°C [Missirlis et al., 2006]. At predetermined time points, the dialysate was sampled and the amount of released doxorubicin was determined using fluorescence spectroscopy (ex; 500 nm, em; 600 nm).

**Cytotoxicity assay**—The CellTiter 96<sup>®</sup> AQ Non-Radioactive Cell Proliferation Assay<sup>(a)</sup> is a colorimetric method used to determine the viability of cells in this cytotoxicity study. ICAM-1 up-regulated A549 cells (80,000 cells/ml) were incubated with cLABL-DOX-NP or DOX-NP for 3 hr and then were washed three times with PBS. Cells were incubated in cell culture medium for 20 hr to allow the sustained release of the drug. For a control experiment, cells were incubated with doxorubicin HCl for 20 hr. After incubation, cells were washed three times with PBS. The solution composed of tetrazolium compound [3-(4,5-dimethylthiazol-2-yl)-5-(3-carboxymethoxyphenyl)-2-(4-sulfophenyl)-2H-tetrazolium, MTS and an electron coupling reagent (phenazine methosulfate; PMS) (20  $\mu$ l) was added into each well containing 100  $\mu$ l of cell culture medium. The plate was then incubated at 37°C, 5% CO<sub>2</sub> for 4 hr. The quantity of formazan product was determined by the amount of 490 nm absorbance.

**Determination of ICAM-1 expression on A549 cells using Enzymed-Linked Immunosorbent Assay (ELISA)**—A549 carcinomic human alveolar basal epithelial cells were cultured in F12K medium with 10% fetal bovine serum (FBS) and 1% Penicillin-Streptomycin (10,000 U/ml) 37°C, 5% CO<sub>2</sub>. Cell monolayers were incubated with TNF- $\alpha$  (1,000 U/ml) or IFN- $\gamma$  (100 U/ml) for 48 hr to activate the up-regulation of ICAM-1 on the cell surface [Konno et al., 2002]. ICAM-1 expression was measured using an indirect ELISA. A549 cells ( $8 \times 10^5$  cells/ml) were seeded in a 96 well-plate. Cells were fixed by using 2% formaldehyde in PBS (100  $\mu$ l/well) and incubated at room temperature for 1 hr. Cells were washed with PBS (200  $\mu$ l/well) and then non-specific adsorption was blocked by incubating with 1% BSA in PBS (120  $\mu$ l/well) for 30 min at room temperature. After washing with PBS, monoclonal anti-human CD54 (ICAM-1) domain D1 (120  $\mu$ l/well) was added and incubated 1 hr at 37°C. Goat anti-mouse IgG HRP (100  $\mu$ l/well) was then added after washing with PBS and incubated for 1 hr at 37°C. Cells were washed three times with PBS and incubated with 3,3',5,5' tetramethylbenzidine as the substrate for 15 min at room temperature. The enzyme-substrate reaction was stopped by adding 1 N sulfuric acid. The absorbance was obtained by UV spectroscopy (Spectramax M5;  $\lambda_{\max}$  450 nm)

**Binding and Uptake of Nanoparticles by A549 cells**—A549 cell monolayers were incubated with TNF- $\alpha$  (1,000 U/ml) for 48 hr to over express ICAM-1 receptors. Cells were then washed three times with serum free F12K and then incubated with nanoparticles (with or without cLABEL conjugated) suspended in serum free medium (0.5 mg/ml). Cells were incubated with nanoparticles for different time intervals to observe the uptake kinetics of particles. After incubation, cells were washed three times with ice-cold PBS and lysed with 0.5% Triton X-100 in 0.2 M NaOH [Davda and Labhasetwar, 2002]. cLABEL-NP and NP associated with the cells were detected and compared using a fluorescence plate reader (Spectramax M5; ex: 450 nm, em: 500 nm) [Koefod and Mann, 1991].

**Inhibition of cLABEL-NP binding to ICAM-1**—Various concentrations of free cLABEL peptide or anti-ICAM-1 mAbs were incubated with activated A549 cells for 30 min, 37°C, 5% CO<sub>2</sub>. Cells were then washed three times with serum free media and incubated with cLABEL-NP or nanoparticles without peptide for 1 hr at the same condition. Cells were washed three times with ice-cold PBS, lysed with 0.5% Triton X-100 in 0.2 M NaOH. cLABEL-NP and NP content bound to the cell surface or internalized into the cells were determined and compared by fluorescence spectroscopy (Spectramax M5; ex: 450 nm, em: 500 nm).

**Intracellular trafficking of cLABEL-NP to lysosomes**—ICAM-1 on A549 cells were activated using (1,000 U/ml) TNF- $\alpha$  for 48 hr. Lysosomes were labeled with Texas Red dextran (10,000 Mw, lysine fixable) to indicate the location of lysosomes. Texas red dextran prepared in serum free F12K (1 mg/ml) was incubated with activated A549 cells for 2 hr. Cells were then washed with serum free media for three times and further incubated with serum free media for up to 12 hr in order to chase the red fluorescent dye to localize in lysosomes [Hirota et al., 2004] and [Duvvuri and Krise, 2005]. Cells were then incubated in the presence of cLABEL-NP or NP containing the green fluorophore, coumarin-6, for 10 min. Cells were washed three times and incubated with serum free medium for each time point. After washing with ice-cold PBS, cells were fixed with 4% formaldehyde solution. Fluorescence emissions of nanoparticles and lysosomes were observed using FITC and rhodamine filter sets, respectively (Nikon Eclipse 80i microscope equipped for epifluorescence). Micrographs were captured using an Orca ER camera (Hamamatsu, Inc., Bridgewater, NJ). Colocalizations of nanoparticles and lysosomes were analyzed by Metamorph, version 6.2 (Universal Imaging Corp., West Chester, PA)



**Intracellular trafficking of doxorubicin and nanoparticles encapsulating doxorubicin**—TNF- $\alpha$  activated A549 cells were incubated with free doxorubicin (0.5 mg/ml) or doxorubicin encapsulated in nanoparticles conjugated with cLABL (cLABL-DOX-NP) or without cLABL (DOX-NP) (3.8 mg/ml) for 1 hr (for 1 hr observation) and 3 hr (for 3 hr, 8 hr and 24 hr observation). Cells were then washed three times with ice-cold PBS and incubated with media with serum for each time period (8 hr and 24 hr). Cells were fixed with 4% paraformaldehyde. Nuclei were labeled with DAPI dilactate (blue) (300 nM, ex: 358 nm, em: 461 nm) for 5 min at 37°C, 5% CO<sub>2</sub>. Micrographs were taken using the Nikon Eclipse microscope.

For some studies, nanoparticles encapsulating doxorubicin contained the fluorophore, coumarin-6, to indicate the location of particles in the cells. cLABL-DOXNP and DOX-NP encapsulating coumarin-6 were incubated with cells for each time period (15 min, 30 min, 1 hr and 3 hr). Cells were washed three times with ice-cold PBS and fixed with 4% paraformaldehyde. Nuclei were labeled with DAPI dilactate (blue) (300 nM, ex: 358 nm, em: 461 nm) for 5 min at 37°C, 5% CO<sub>2</sub>. Micrographs were taken using the Nikon Eclipse microscope.

**Statistical analysis**—Statistical evaluation of data was performed using an analysis of variance (one-way ANOVA). Newman–Keuls was used as a post-hoc test to assess the significance of differences. To compare the significance of the difference between the means of two groups, the *t*-test was performed; in all cases, a value of  $p < 0.05$  was accepted as significant.

### 3. Results and Discussion

#### Preparation of Carboxylated Pluronic® F-127

The hydroxyl groups of Pluronic® F-127, HO(C<sub>2</sub>H<sub>4</sub>O)<sub>100</sub>(C<sub>3</sub>H<sub>6</sub>O)<sub>65</sub>(C<sub>2</sub>H<sub>4</sub>O)<sub>100</sub>H [Kabanov et al., 2002], were converted to carboxyl groups to facilitate the conjugation reaction of this surfactant with the terminal amine of cLABL peptide. The <sup>1</sup>H NMR spectrum displayed the absorption of methylene protons adjacent to the succinic moiety at  $\delta = 4.1$  ppm and the proton of the carboxylic acid at  $\delta = 12$  ppm (Supplementary Fig. 1) [Guerrouache et al., 2006]. The COOH formation was confirmed by FTIR spectroscopy. The FTIR spectrum showed a strong C=O stretching absorption at 1,720 cm<sup>-1</sup> and a very broad, strong absorption at 3,500 cm<sup>-1</sup>, which indicated the appearance of the hydroxyl of carboxylic acid (Supplementary Fig. 2). These results confirmed the formation of carboxylated Pluronic® F-127.

#### Preparation of PLGA nanoparticles encapsulating coumarin-6

PLGA nanoparticles were prepared by a spontaneous solvent displacement method using carboxylated Pluronic® F-127 as an anionic surfactant. Dynamic light scattering showed that the size of nanoparticles encapsulating coumarin-6 was approximately 225 nm in diameter with a low polydispersity suggesting a narrow size distribution, and that the zeta potential value was about -45 mV (Table 1). An increase in size and negative charge of nanoparticles after conjugation with cLABL peptide was observed, which was expected due to the pI value of cLABL peptide (pI=3.5). The size and charge of nanoparticles encapsulating coumarin-6 were comparable when either form of PLGA (0.22 dl/g or 0.67 dl/g) was used to formulate nanoparticles. The encapsulation efficiencies of coumarin-6 in both nanoparticles were reported in Table 2. As expected, the encapsulation efficiencies were diminished in both types of PLGA after the conjugation reaction.

## Preparation of PLGA nanoparticles encapsulating doxorubicin

A variety of mAbs have been identified for immunotherapy against a wide range of cancers [Kurosawaa et al., 2008]. Peptides that can target the immunoglobulin receptor offer a simple alternative to mAbs. The cLABL peptide itself has a therapeutic effect, however, potency may be improved by using this ligand to target drug loaded nanoparticles. Nanocarriers often exhibit various benefits such as prolonged circulation and tumor localization via the enhanced permeability and retention effect [Kim et al., 2008]. Doxorubicin, one of the most widely used anti-cancer drugs, was incorporated in nanoparticles in this study.

Nanoparticles encapsulating doxorubicin was prepared and characterized in this study. The size and charge of doxorubicin loaded nanoparticles increased after conjugation with the cLABL peptide (Table 1). The encapsulation efficiency of doxorubicin in nanoparticles was acceptable at  $41 \pm 4.8\%$  and  $51 \pm 7.6\%$  when PLGA Mw~20 KDa and ~90 KDa were used to formulate nanoparticles, respectively (Table 2). After the conjugation reaction, the encapsulation efficiency was reduced by ~54 and ~47% when PLGA Mw~20 KDa and ~90 KDa were reacted with cLABL, respectively. However, other studies have suggested that the encapsulation efficiency may be increased by an ester linkage of the carboxylic acid end group of PLGA and the hydroxyl group of doxorubicin, which results in retention of doxorubicin during the nanoparticle preparation procedure [Yoo et al., 2000]. Ultimately, doxorubicin serves as a convenient fluorescent marker for these studies and more hydrophobic drugs would likely offer improved encapsulation efficiencies.

## Conjugation of cLABL peptide on the surface of nanoparticles

The efficiency of the coupling reaction between the amino group of cLABL and the carboxyl of Pluronic<sup>®</sup> F-127-COOH coated on nanoparticles was determined. The amounts of free cLABL were analyzed (prior to and after the reaction) by reversed phase HPLC. The peptide density on the surface of nanoparticles encapsulating coumarin-6 was calculated from the total surface area assuming a normal Guassian particle size distribution [Zhang et al, 2008] The density of peptide on both types of nanoparticle surfaces (0.22 dl/g and 0.67 dl/g) were comparable (Table 3). The calculation showed a higher density of cLABL conjugated compared to previous studies [Zhang et al., 2008] which conjugated the peptide with polyethylene glycol (PEG)-modified poly(ethylene-alt-maleic acid) on the nanoparticle surface. This may be due to the more available carboxyl groups of Pluronic<sup>®</sup> -COOH coated on the nanoparticle surface. Therefore, the use of modified Pluronic<sup>®</sup> may reduce the steps of the conjugation reaction, and also increase the density of peptide conjugated [Zhang et al. 2008].

## *In vitro* drug release study of nanoparticles encapsulating doxorubicin

Generally the release of doxorubicin from the drug carriers was pH dependent probably due to the increase in solubility of doxorubicin at mildly acidic pH [Gillies and Frechet, 2005] and [Kataoka et al., 2000]. The release of the drug at pH 4 and 7.4 were determined for doxorubicin encapsulated in cLABL-NP and untargeted NP. These pH values were selected to represent extracellular and lysosomal pH values. The drug release from PLGA nanoparticles was determined using PLGA inherent viscosity 0.67 dl/g in acetate buffer at pH 4 and phosphate buffer at pH 7.4. The release of doxorubicin from cLABL-DOX-NP followed a biphasic profile regardless of pH (Fig 8). The release profile was characterized by a rapid release in the initial stage. The release of doxorubicin began with an initial burst of  $35 \pm 1.7\%$  and  $34 \pm 2.8\%$  from cLABL-DOX-NP at pH 4 and 7.4, respectively, in the first three hours of the study. Drug burst may result from the large surface to volume ratio of nanoparticles and from rapid loss of drug via diffusion through the polymer matrix at or near the particle surface. The initial burst phase was followed by slow and sustained release. The slower phase likely resulted from continued diffusion through the PLGA matrix [Holgado et al., 2008].

A higher amount of doxorubicin was released from unmodified PLGA nanoparticles at pH 4 compared to at pH 7.4. The release profile of the drug from NP without peptide showed a greater initial burst at pH 4 and pH 7.4 in a comparison to the conjugated peptide, i.e.,  $76 \pm 4.4\%$  vs  $35 \pm 1.7\%$  and  $53 \pm 2.7\%$  vs  $34 \pm 2.8\%$ , respectively, in first three hours. The rapid release at the initial state may be due to the high aqueous solubility of the protonated form of doxorubicin at the glycosidic amine in a low pH medium [Gillies and Frechet, 2005] and [Kataoka et al., 2000]. Interestingly, doxorubicin was released from cLABL-NP in a higher amount in higher pH medium (pH 7.4) compared with medium pH 4 as shown in Fig. 8. The more increasing release of doxorubicin from cLABL-DOX-NP in higher basic pH may have resulted from the agglomeration of the nanoparticles during the release study at pH 4. At higher pH, cLABL has higher negatively charge compared to at more acidic pH (pI~3.5). The high amount of doxorubicin released at this pH should be considered for drugs delivered by this nanoparticle formulation. The cLABL-NP would need to rapidly localize to the lung epithelium expressing ICAM-1 to avoid premature drug release supporting the pulmonary delivery as a choice of the route of administration. Furthermore, selection of more hydrophobic chemotherapeutic agents may be appropriate.

### Cytotoxicity assay

The cytotoxicity of doxorubicin HCl, cLABL-DOX-NP and DOX-NP to A549 cells was evaluated by using MTS assay. The  $IC_{50}$  value of free doxorubicin, doxorubicin released from cLABL-NP and doxorubicin released from unconjugated NP was 60, 30 and 53  $\mu\text{g/ml}$ , respectively. The cytotoxicity of doxorubicin released from nanoparticles was comparable to that of free doxorubicin. The concentrations of doxorubicin in nanoparticles were calculated from the drug loading adjusted by the encapsulation efficiency. The relative  $IC_{50}$  value of doxorubicin from each formulation suggested that the activity of drug encapsulated in nanoparticles were not affected by the encapsulation and conjugation reaction. The  $IC_{50}$  values of cLABL-DOX-NP and DOX-NP were 3.1 and 3.3  $\text{mg/ml}$ , respectively. PLGA NP without doxorubicin did not show any cytotoxicity up to 10  $\text{mg/mL}$  (data not shown) suggesting that the doxorubicin is slowly released from these non-cytotoxic carriers. Modification of PLGA NPs with cLABL did not negatively affect the cell viability.

### Uptake and Internalization of Nanoparticles

Pro-inflammatory cytokines such as TNF- $\alpha$  have previously been shown to upregulate the expression of ICAM-1 [Konno et al., 2002]. Incubating A549 cells with TNF- $\alpha$  (1,000 U/ml) or IFN- $\gamma$  (100 U/ml) resulted in about 5 fold and 4 fold increase of ICAM-1, respectively, as determined by ELISA (Fig. 1). This result confirmed the overexpressed of ICAM-1 and validated the use of this cell line as an inflammatory epithelial cell model. The binding and uptake of cLABL-NP to A549 cells were found to be significantly more rapid compared to untargeted NP. The increasing fluorescence intensity demonstrated the increasing amount of nanoparticles bound or taken up by cells (Fig. 2). In the presence of cLABL-NP, the fluorescence intensity was 2.3 fold higher compared to the control nanoparticles after 5 min of incubation. The difference in the uptake extent diminished when the incubation time increased. This result may indicate saturation of ICAM-1 receptors. In addition, A549 cells have been shown to endocytose nanoparticles extensively, which may explain the significant uptake of unlabeled nanoparticles [Kimberly and Kenneth, 2001].

A blocking study demonstrated the inhibition of cLABL-NP binding to ICAM-1 by free cLABL and anti-ICAM-1 mAbs. The depletion of fluorescence intensity showed that the binding of cLABL-NP to ICAM-1 was impeded when free cLABL was incubated with cells first (Fig. 3A) suggesting a specific binding of cLABL-NP to ICAM-1 on A549 cells [Muro et al., 2005]. In addition, a decrease in fluorescent intensity was shown when anti-ICAM-1 was pre-incubated with the cells; however, the difference was not statistically significant (Fig. 3B).



### Intracellular trafficking of cLABEL-NP to lysosomes

The cLABEL-NPs were observed to rapidly internalize into A549 cells after the 15 min incubation period. This rapid internalization of ICAM-1 targeting nanoparticles agreed with internalization of nanocarriers targeted using anti-ICAM-1 monoclonal antibodies studied by Muro et al (15-30 min) [Muro et al., 2003]. The binding and internalization of cLABEL-NP were likely induced by the multimeric nature of ICAM-1 ligands (cLABEL) on the nanoparticle surface [Muro et al., 2003]. In this study, cLABEL-NPs were observed to accumulate in lysosomes at 1 hr after binding to the cell surface. Subsequently, the colocalization of cLABEL-NP with lysosomes steadily decreased until no colocalization was observed at 24 hr (Fig. 4).

The intracellular trafficking kinetics of cLABEL-NP may have advantages in comparison to unconjugated NP or free drug. Muro et al. report that the cLABEL-NP spend more time in the early endosomes as described in the trafficking study of anti-ICAM-1 nanoparticles into HUVECs. [Muro et al., 2003]. The result in this study revealed that internalized cLABEL-NP may traffic away from lysosomes. The removal of cLABEL-NP, from lysosomes was probably not due to disruption of the lysosomes because there was no change in the distribution of Texas Red conjugated dextran during 24 hr of incubation observed in this study [Panyam et al., 2002]. Overall, the results suggested that the lysosomal degradation of cLABEL-NP may be less pronounced by this intracellular trafficking pathway. The therapeutic activity of cytotoxic drugs may also be prolonged by avoiding enzymatic degradation in the lysosomes by lysosomal sequestration.

Untargeted nanoparticles merged with lysosomes at 2 hr after incubation but to a lower extent compared to ICAM-1 targeted NPs (Fig. 5). This result suggested that nanoparticles without peptide may be taken up more slowly than targeted NP which agrees with the result of our uptake study described above. The accumulation of untargeted NPs was also not observed at a later time point of incubation. A mechanism of escape of PLGA-NP has been proposed previously by the fact that PLGA-NP may undergo charge neutralization during trafficking [Panyam et al., 2002]. The removal of particle charge was suggested to mediate membrane association leading to the escape of nanoparticles [Panyam et al., 2002].

### Intracellular trafficking of doxorubicin and cLABEL-NP encapsulating doxorubicin

The cLABEL-DOX-NP and DOX-NP were incubated with A549 cells to study intracellular trafficking. Intracellular localization of free doxorubicin, cLABEL-DOX-NP and DOX-NP were investigated using fluorescence microscopy. Free doxorubicin, which is fluorescent (red), was used as a control. The nuclei of cells were stained with the blue fluorescence dye, DAPI. The photographs of cLABEL-DOX-NP, DOX-NP and free doxorubicin were combined with the stained nuclei to observe the colocalization of the doxorubicin and the nuclei. The merged micrographs showed that free doxorubicin displayed rapid colocalization with the nuclei of A549 cells (in 1 hr) as expected (Fig. 6A). Cells exposed to cLABEL-DOX-NP exhibited a small degree of colocalization of doxorubicin and nuclei in some cells during the first hour of the study (Fig. 6B). This result suggested that a small amount of doxorubicin may be released and localized in the nuclei as indicated by the faint purple color in the nuclei. The colocalization of the drug and the nuclei shown from the color combination was further observed until 24 hr. In contrast, this colocalization of doxorubicin and the nuclei was observed at later time (3 hr) for the untargeted NP (Fig.6C). Doxorubicin was also observed to localize within the nuclei until 24 hrs. In a comparison to free doxorubicin, doxorubicin encapsulated in nanoparticles was slowly released and localized in the nuclei more gradually after cellular uptake. This result provided evidence to the capability of nanoparticles to offer targeted, intracellular delivery of this cytotoxic drug and suggested the prolonged retention of doxorubicin and sustained release of drug from nanoparticles.

Also, the yellow dots in overlaid pictures of cLABL-NP or NP (green) and doxorubicin (red) confirmed the retention of doxorubicin in nanoparticles encapsulating coumarin (green) (Fig. 7A and B). The colocalization of dye and drug suggested that the images show the uptake of nanoparticles containing drug and not released drug.

#### 4. Conclusion

This work has aimed to further develop the role of cLABL as a means of targeting PLGA NP to a molecular marker, ICAM-1, associated with inflammatory diseases and cancer. Targeted nanoparticles are of increasing interest because they may allow a reduction of adverse side effects and increase the efficacy of a drug by localizing it to the desired site of action. PLGA has advantages over other polymers due to its biodegradability, biocompatibility and approval by the FDA. Besides, PLGA NPs have provided controlled drug release in several studies, which lowered observed side effects [Avgoustakis, 2004], [Keegan et al., 2004], [Kim et al., 2008] and [Panyam et al., 2002]. Here, PLGA nanoparticles targeting the immunologically active receptor, ICAM-1, were formulated by attaching the cLABL peptide to the nanoparticle surface. The cLABL-NP displayed specific binding to ICAM-1 compared to non-targeted NP. The cLABL-NPs were also more rapidly taken into A549 lung epithelial cells induced to overexpress ICAM-1. Intracellular trafficking studies showed that cLABL-NP accumulated in lysosomes for 1 hr and then left after 3 hr. Conversely, untargeted NP accumulated in lysosomes more slowly (2 hr), and also left at a later time point. cLABL-NP encapsulating doxorubicin also accumulated quickly in A549 cells. Drug release studies indicated that the cLABL-NP formulated with a high Mw PLGA exhibited sustained drug release that depended on pH. Finally, the cytotoxicity study of cLABL-NP and NP compared to free doxorubicin HCl showed similar  $IC_{50}$  values suggesting that the activity of the drug released from nanoparticles was retained. These studies verified that cLABL can target nanoparticles to lung epithelial cells to deliver chemotherapeutics and provide controlled release drug delivery. The effectiveness of targeted delivery *in vivo* must be inquired in future studies.

#### Supplementary Material

Refer to Web version on PubMed Central for supplementary material.

#### Acknowledgments

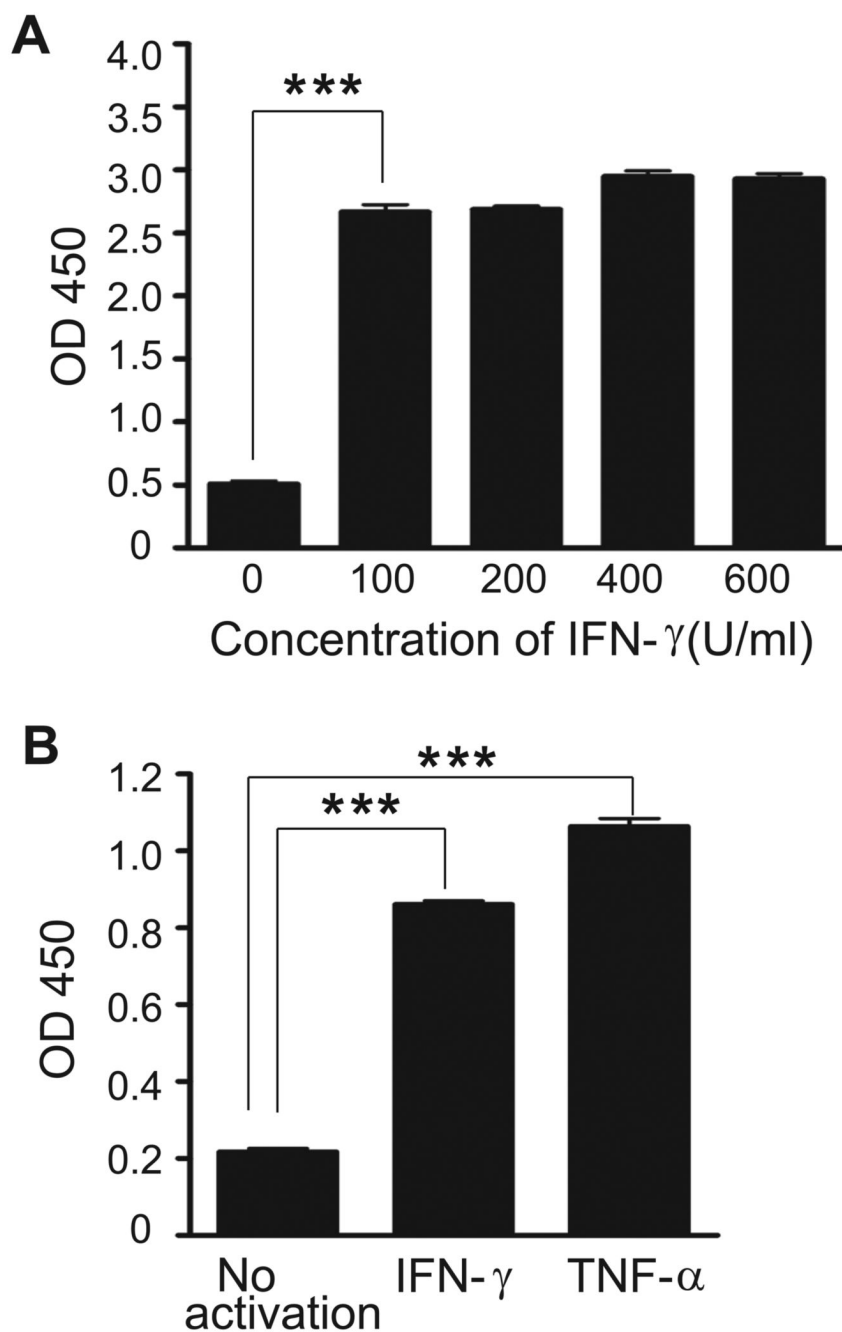
The authors acknowledge Prof. Russell Middaugh for the use of equipment, Prof. Jeffrey Krise for providing the fluorescence microscope and DAPI dilactate and graduate students in the laboratories of Prof. Jeffery Krise and Prof. Teruna Siahaan for technical assistance. We also appreciate Prof. Laird Forrest for providing doxorubicin HCl. We would like to acknowledge support from the Cystic Fibrosis Foundation, the Coulter Foundation, and the Higuchi Biosciences Center as well as additional lab funding from the American Heart Association, the NIH (R03 AR054035, P20 RR016443 and T32 GM08359-11) and the Department of Defense. In addition, we acknowledge the support of the NSF (CHE 0719464).

#### References

1. Adams PG, Weiner ML. Monoclonal antibody therapy of cancer. *Nature biotechnology* 2005;23:1147–1157.
2. Anderson ME, Siahaan TJ. Mechanism of binding and internalization of ICAM-1-derived cyclic peptides by LFA-1 on the surface of T cells: a potential method for targeted drug delivery. *Pharm Res* 2003;20:1523–1532. [PubMed: 14620502]
3. Anderson ME, Siahaan TJ. Targeting ICAM-1/LFA-1 interaction for controlling autoimmune diseases: designing peptide and small molecule inhibitors. *Peptides* 2003;24:487–501. [PubMed: 12732350]
4. Anderson ME, Yakovela T, Hu Y, Siahaan TJ. Inhibition of ICAM-1/LFA-1-mediated heterotypic T cell adhesion to epithelial cells: design of ICAM-1 cyclic peptides. *Bioorganic & Medicinal Chemistry Letters* 2004;14:1399–1402. [PubMed: 15006370]

5. Avgoustakis K. Pegylated poly(Lactide) and poly(Lactide-Co-Glycolide) nanoparticles: preparation, properties and possible applications in drug delivery. *Current Drug Delivery* 2004;1:321–333. [PubMed: 16305394]
6. Cheng J, Teply BA, Sherifi I, Sung J, Luther G, Gu FX, Levy-Nissenbaum E, Radovic-Moreno AF, Langer R, Farokhzad OC. Formulation of functionalized PLGA-PEG nanoparticles for *in vivo* targeted drug delivery. *Biomaterials* 2007;28:869–876. [PubMed: 17055572]
7. Davda J, Labhasetwar V. Characterization of nanoparticle uptake by endothelial cells. *International Journal of Pharmaceutics* 2002;233:51–59. [PubMed: 11897410]
8. Duneahoo AL, Anderson M, Majumdar S, Kobayashi N, Berkland C, Siahaan TJ. Cell adhesion molecules for targeted drug discovery. *J Pharm Sci* 2006;95:1856–1872. [PubMed: 16850395]
9. Duvvuri M, Krise JP. A novel assay reveals that weakly basic model compounds concentrate in lysosomes to an extent greater than pH-partitioning theory would predict. *Mol. Pharm* 2005;2:440–448. [PubMed: 16323951]
10. Gillies ER, Frechet JMJ. pH-responsive copolymer assemblies for controlled release of doxorubicin. *Bioconjugate Chem* 2005;16:361–368.
11. Guerrouache M, Karakasyan C, Gaillet C, Canva M, Millot MC. Immobilization of a functionalized poly(ethylene glycol) onto  $\beta$ -cyclodextrin-coated surfaces by formation of inclusion complexes: application to the coupling of proteins. *J Applied Polym Sci* 2006;100:2362–2370.
12. Hirota Y, Masuyama N, Kuronita T, Fujita H, Himeno M, Tanaka Y. Analysis of post-lysosomal compartments. *Biochemical and biophysical. Research Communications* 2004;314:306–312.
13. Holgado MA, Arias JL, Cozar MJ, Alvarez-Fuentes J, Ganan-Calvo AM, Fernandez-Arevalo M. Synthesis of lidocaine-loaded PLGA microparticles by flow focusing effects on drug loading and release properties. *International Journal of Pharmaceutics* 2008;358:27–35. [PubMed: 18372128]
14. Hopkins AM, Baird AW, Nusrat A. ICAM-1: targeted docking for exogenous as well as endogenous ligands. *Adv. Drug. Deliv. Rev* 2004;56:763–778. [PubMed: 15063588]
15. Huang M, Matthews K, Siahaan TJ, Kevil CG.  $\alpha_1$ -Integrin I domain cyclic peptide antagonist selectively inhibits T cell adhesion to pancreatic islet microvascular endothelium. *Am J Physiol Gastrointest Liver Physiol* 2005;288:G67–G73. [PubMed: 15319185]
16. Kabanov AV, Lemieux P, Vinogradov S, Alakhov V. Pluronic<sup>®</sup> block copolymers: novel functional molecules for gene therapy. *Advanced Drug Delivery Reviews* 2002;54:223–233. [PubMed: 11897147]
17. Kataoka K, Matsumoto T, Yokoyama M, Okano T, Sakurai Y, Fukushima S, Okamoto K, Kwon GS. Doxorubicin-loaded poly(ethylene glycol)-poly( $\beta$ -benzyl-L-aspartate) copolymer micelles: their pharmaceutical characteristics and biological significance. *J controlled release* 2000;64:143–153.
18. Keegan ME, Falcone JL, Leung TC, Saltzman WM. Biodegradable microspheres with enhanced capacity for covalently bound surface ligands. *Macromolecules* 2004;37:9779–9784.
19. Kim J, Lee JE, Lee SH, Yu JH, Lee JH, Park TG, Hyeon T. Designed fabrication of a multifunctional polymer nanomedical platform for simultaneous cancer targeted imaging and magnetically guided drug delivery. *Adv. Mater* 2008;20:478–483.
20. Kimberly AF, Yazdani M, Kenneth LA. Microparticulate uptake mechanisms of in-vitro cell culture models of the respiratory epithelium. *JPP* 2001;53:57–66.
21. Koefod RS, Mann KR. Common emissive intermediates in the thermal and photochemical reactions of nonemissive cyclopentadienylruthenium (II) complexes of coumarin laser dyes. *Inorg. Chem* 1991;30:221–228.
22. Konno S, Grindle KA, Lee W, Schroth MK, Mosser GA, Brockman-Schneider RA, Busse WW, Gern JE. Interferon- $\beta$  enhances rhinovirus-induced RANTES secretion by airway epithelial cells. *Am. J Respir Cell Mol Biol* 2002;26:594–601. [PubMed: 11970912]
23. Kurosawaa G, Akahoria Y, Moritaa M, Sumitomb M, Satoc N, Muramatsub C, Eguchib K, Matsudab K, Takasakid A, Tanaka M, Ibaa Y, Hamada-Tsutsumia S, Ukaie Y, Shiraishie M, Suzukie K, Kurosawaa M, Fujiiyama S, Takahashif N, Katog R, Mizoguchih Y, Shamotoi M, Tsudaj H, Sugiurak M, Hattoril Y, Miyakawal S, Shirokic R, Hoshinagac K, Hayashid N, Sugiokal A, Kurosawaa Y. Comprehensive screening for antigens overexpressed on carcinomas via isolation of human mAbs that may be therapeutic. *PNAS* 2008;105:7287–7292. [PubMed: 18474866]

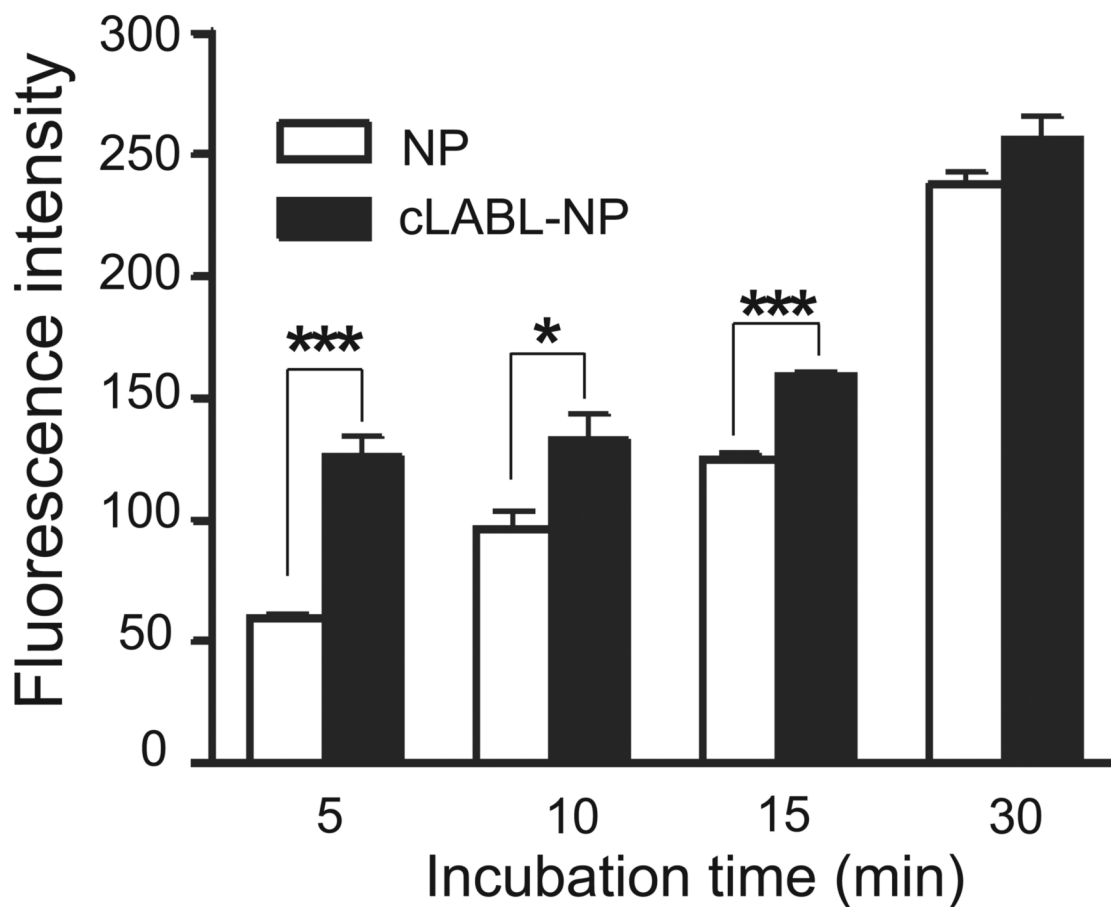
24. McDawa A, Leitinger B, Stanley P, Bates PA, Randi AM, Hogg N. The I domain of integrin leukocyte function associated antigen-1 is involved in a conformational change leading to high affinity binding to ligand intercellular adhesion molecule 1 (ICAM-1). *J Biol Chem* 1998;273:27396–27403. [PubMed: 9765268]
25. Melis M, Spatafora M, Melodia A, Pace E, Gjomarkaj M, Merendino AM, Bonsignore G. ICAM-1 expression by lung cancer cell lines: effects of upregulation by cytokines on the interaction with LAK cells. *Eur Respir J* 1996;9:1831–1838. [PubMed: 8880099]
26. Missirlis D, Kawamura R, Tirelli N, Hubbel JA. Doxorubicin encapsulation and diffusional release from stable, polymeric, hydrogel nanoparticles. *European journal of pharmaceutical sciences* 2006;29:120–129. [PubMed: 16904301]
27. Muro S, Cui X, Gajewski C, Murciano JC, Myzykantor VR, Koval M. Slow intracellular trafficking of catalase nanoparticles targeted to ICAM-1 protects endothelial cells from oxidative stress. *Am. J. Physiol.: Cell Physiol* 2003;285:C1339–C1347. [PubMed: 12878488]
28. Muro S, Gajewski C, Koval M, Muzykantor VR. ICAM-1 recycling in endothelial cells: a novel pathway for sustained intracellular delivery and prolonged effects of drugs. *Blood* 2005;105:650–658. [PubMed: 15367437]
29. Panyam J, Zhou W, Prabha A, Sahoo SK, Labhasetwar V. Rapid endo-lysosomal escape of poly(DL-lactide-co-glycolide) nanoparticles: implications for drug and gene delivery. *FASEB journal* 2002;16:1217–1226. [PubMed: 12153989]
30. Tibetts SA, Jois DSS, Siahaan TJ, Benedict SH, Chan MA. Linear and cyclic LFA-1 and ICAM-1 peptides inhibit T cell adhesion and function. *Peptides* 2000;21:1161–1167. [PubMed: 11035201]
31. Wofsy D. Strategies for treating autoimmune disease with monoclonal antibodies. *West J Med* 1985;143:804–809. [PubMed: 3911593]
32. Wojcikiewicz EP, Zhang X, Chen A, Moy VT. Contributions of molecular binding events and cellular compliance to the modulation of leukocyte adhesion. *JCS* 2003;116:2531–2539.
33. Yoo HS, Lee KH, Oh JE, Park TG. *In vitro* and *in vivo* anti-tumor activities of nanoparticles based on doxorubicin-PLGA conjugates. *J Control Rel* 2000;68:419–431.
34. Yusuf-Makagiansar H, Anderson ME, Yakovleva TV, Murray JS, Siahaan TJ. Inhibition of LFA-1/ICAM-1 and VLA-4/VCAM-1 as a therapeutic approach to inflammation and autoimmune diseases. *Medicinal Research Reviews* 2002;22:146–167. [PubMed: 11857637]
35. Yusuf-Makagiansar H, Makagiansar IT, Hu Y, Siahaan TJ. Synergistic inhibitory activity of  $\alpha$ - and  $\beta$ -LFA-1 peptides on LFA-1/ICAM-1 interaction. *Peptides* 2001;22:1995–1962.
36. Yusuf-Makagiansar H, Siahaan TJ. Binding and internalization of an LFA-1-derived cyclic peptide by ICAM receptors on activated lymphocyte: a potential ligand for drug targeting to ICAM-1-expressing cells. *Pharmaceutical Research* 2001;18:329–335. [PubMed: 11442273]
37. Yusuf-Makagiansar H, Yakovleva TV, Tejo BA, Jones K, Hu Y, Verkhivker GM, Audus KL, Siahaan TJ. Sequence recognition of  $\alpha$ LFA-1-derived peptides by ICAM-1 cell receptors: inhibitors of T-cell adhesion. *Chem Biol Drug Des* 2007;70:237–246. [PubMed: 17718718]
38. Zhang N, Chittasupho C, Duangrat C, Teruna SJ, Berkland C. PLGA nanoparticle-peptide conjugate effectively targets intercellular cell-adhesion molecule-1. *Bioconjugate Chem* 2008;19:145–152.



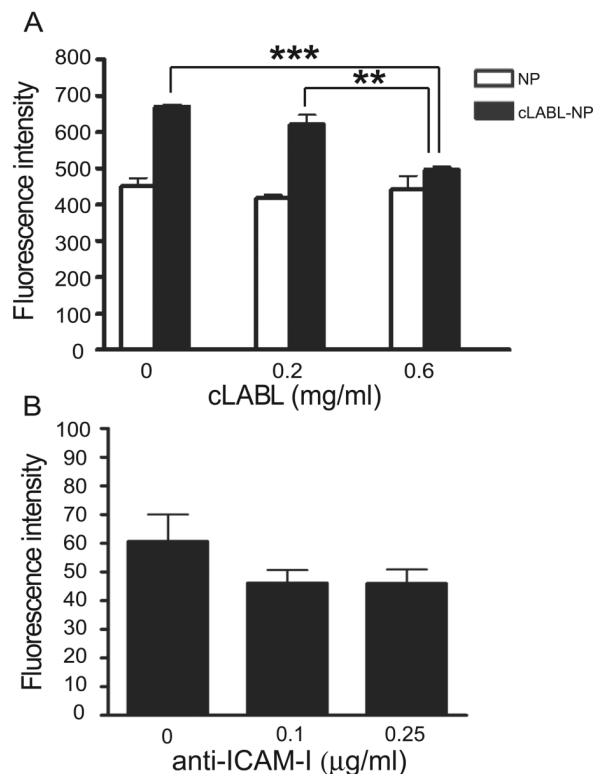
**Fig. 1.**

(A). Effect of IFN- $\gamma$  on A549 ICAM-1 expression. Confluent monolayers of A549 cells were incubated 48 hr with IFN- $\gamma$  (0-600 U/ml), and ICAM-1 expression was determined by ELISA. Data were presented as mean  $\pm$  S.D. (n = 3). (B) Expression of ICAM-1 activated by TNF- $\alpha$  (1,000 U/ml) was significantly higher than IFN- $\gamma$  (100 U/ml) and non-activated A549 cells. Data are presented as mean  $\pm$  S.D. (n = 3). \*\*\* indicates  $p < 0.001$ .

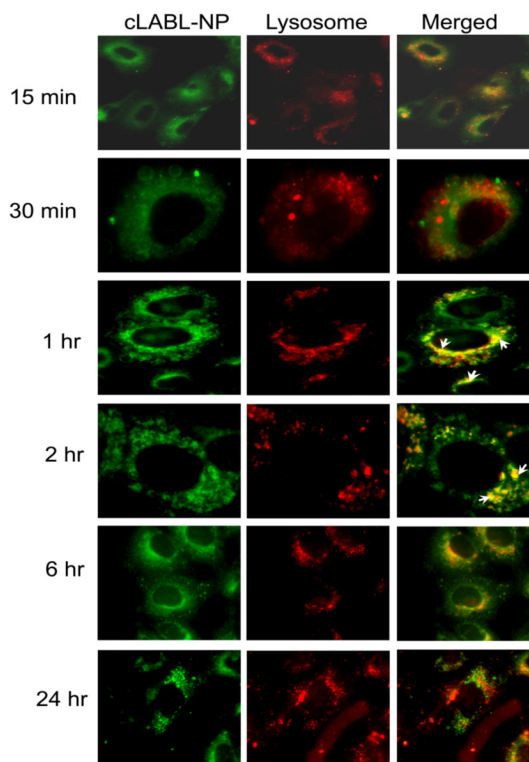




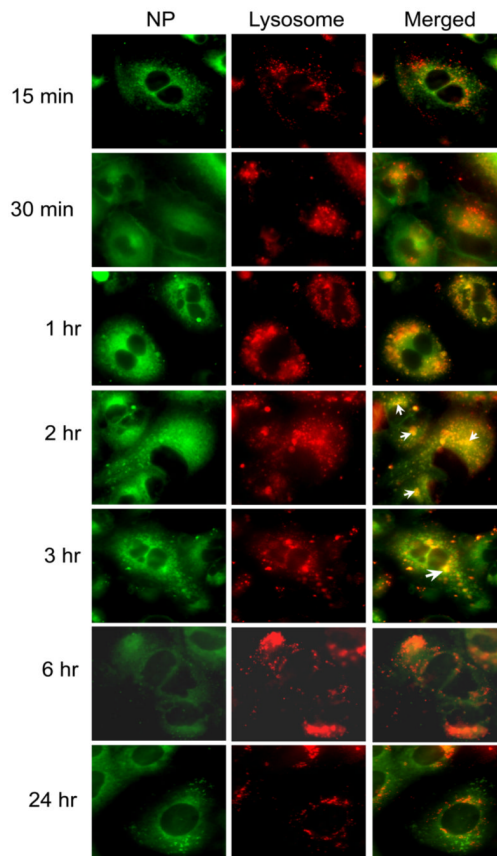
**Fig. 2.** Fluorescent intensity of cLABL-NP was significantly higher than untargeted NP for short incubation periods. Cells were incubated with nanoparticles (0.5 mg/ml) for different time intervals to observe the uptake of particles. Cell lysates were analyzed by fluorescence spectroscopy and data presented are mean  $\pm$  S.D. (n = 3). \*\*\* indicates  $p < 0.001$  and \* indicates  $p < 0.05$ .



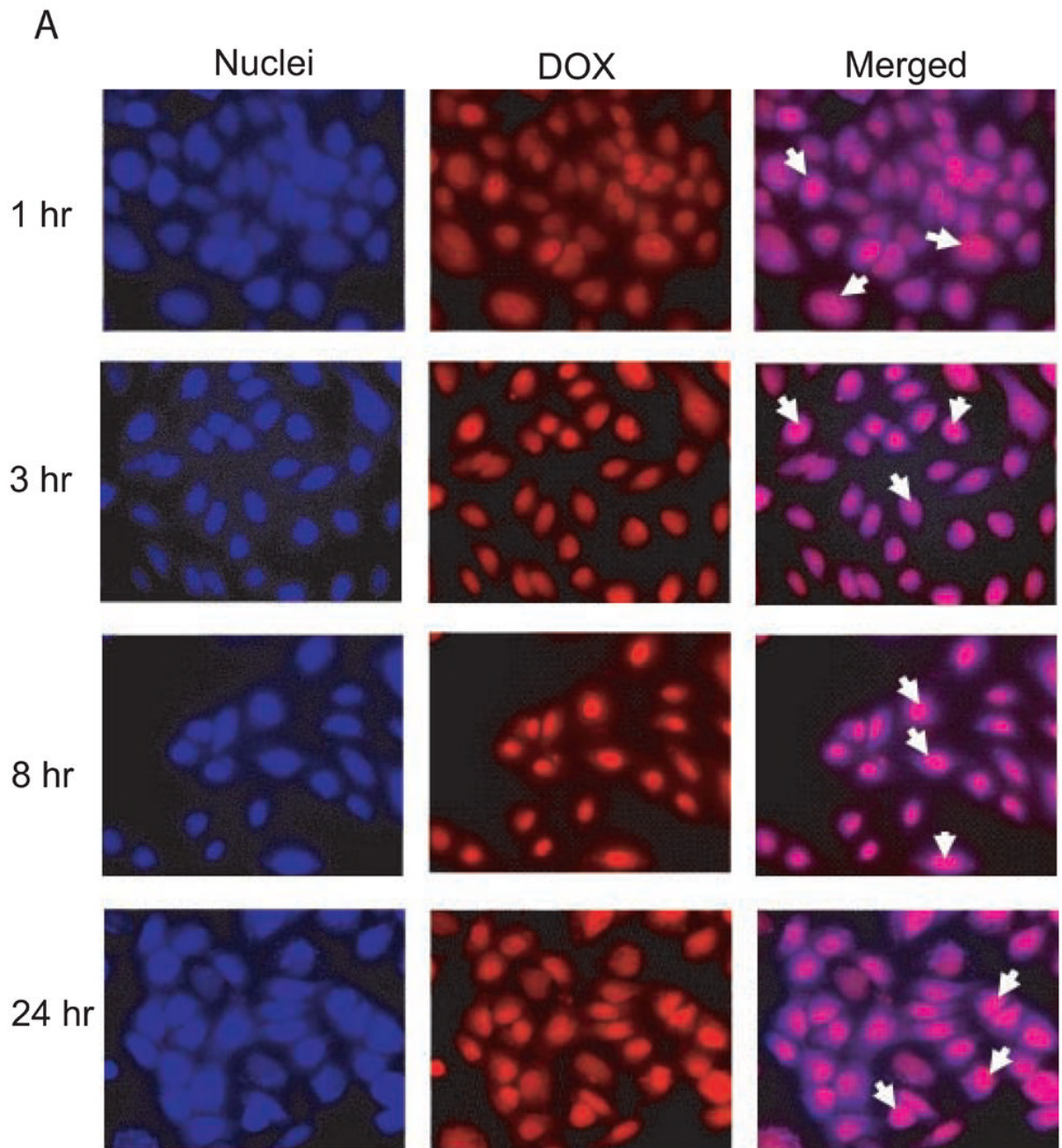
**Fig. 3.** (A). The depletion of fluorescence intensity showed the inhibition of cLABL to the binding and internalization of cLABL-NP. Free cLABL peptide was incubated with cells for 30 min. Cells were then washed and incubated with nanoparticles for 1 hr. Cell lysates were analyzed by fluorescence spectroscopy and data presented are mean  $\pm$  S.D. ( $n = 3$ ). (B) Anti-ICAM-1 pre-incubated with cells reduced the fluorescent intensity but the difference was not statistically significant. Cells were treated with anti-ICAM-1 for 30 min, and then incubated with nanoparticles for 1 hr. Cell lysates were analyzed by fluorescence spectroscopy and data presented are the mean  $\pm$  S.D. ( $n = 3$ ). \*\*\* indicates  $p < 0.001$  and \*\* indicates  $p < 0.01$ .



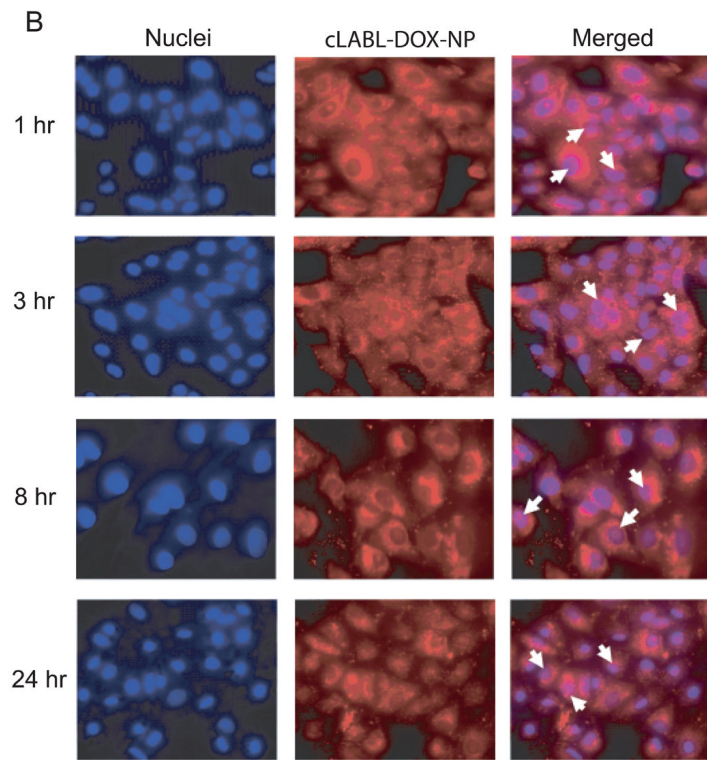
**Fig. 4.** Localization of cLABL-NP with lysosomes (red) was observed at 1 hr after incubation with cells. The extent of colocalization decreased thereafter. Cells were incubated in the presence of cLABL-NP for 10 min, washed and incubated with serum free medium for each time point. Selected colocalizations of NP and lysosomes are indicated by the white arrows.

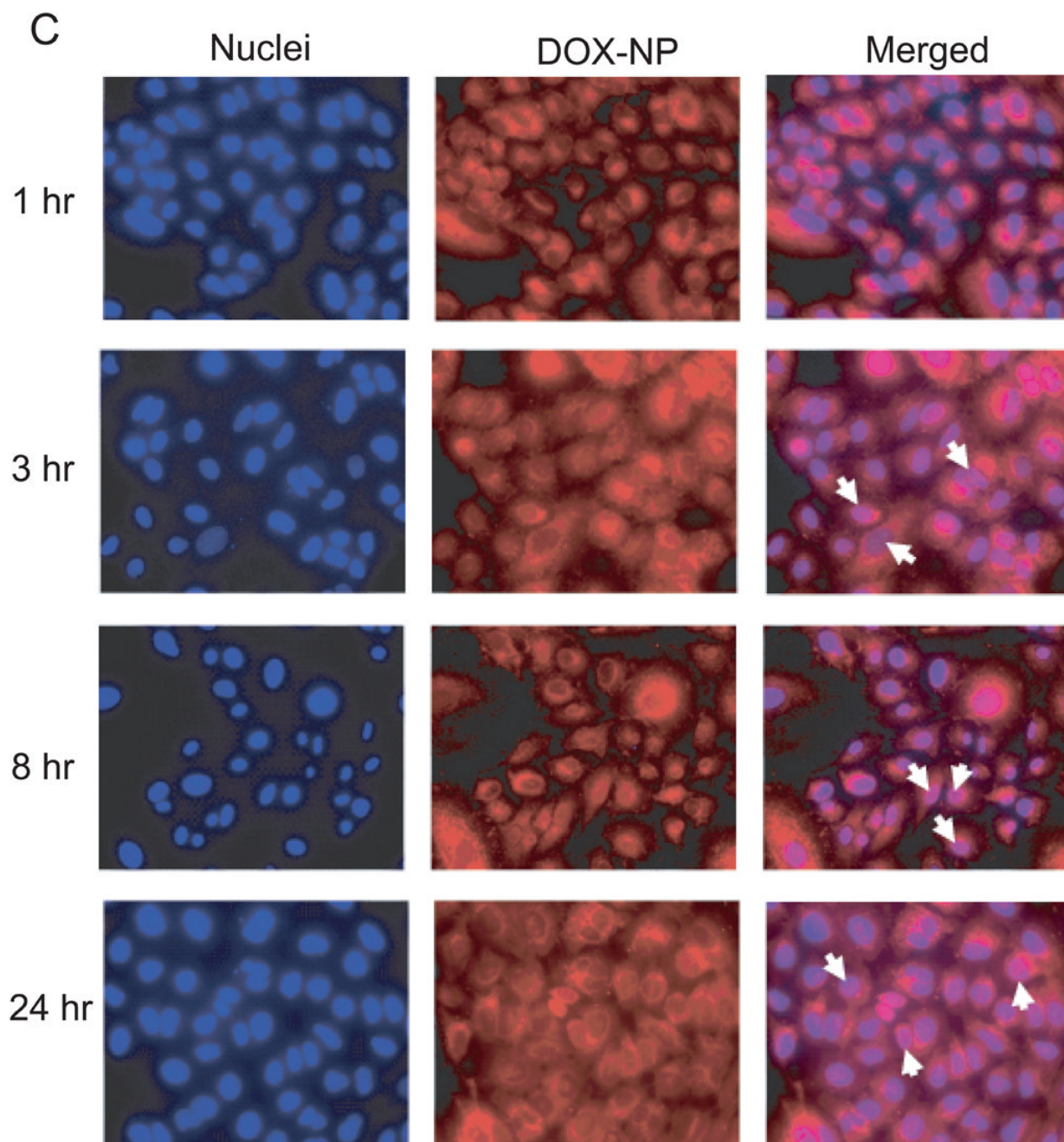


**Fig. 5.** Colocalization of untargeted NP with lysosomes was greatly decreased compared to ICAM-1 targeted NP. Selected colocalizations of NP and lysosomes are indicated by the white arrows.





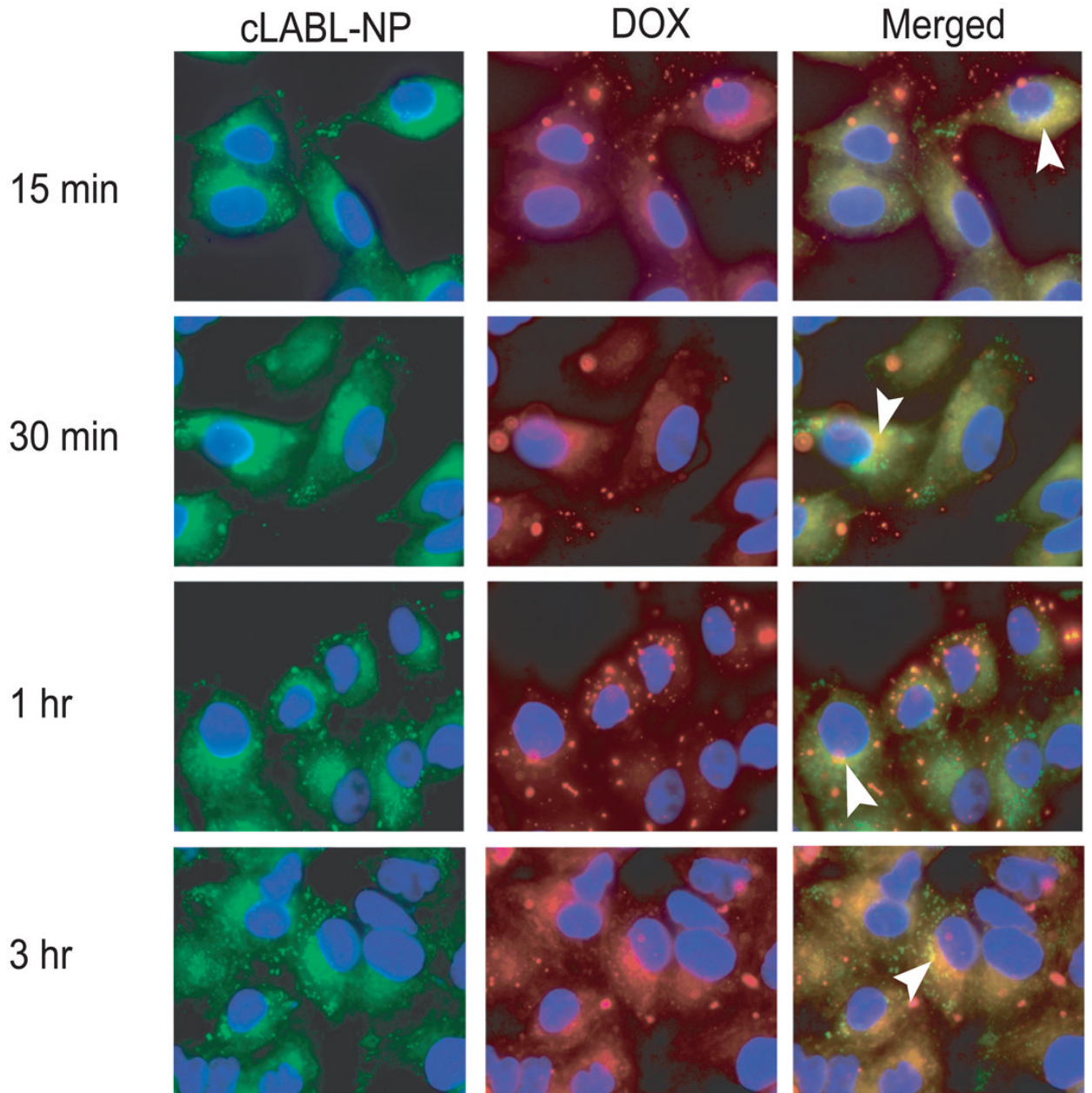




**Fig. 6.**

(A) The colocalization of doxorubicin HCl and the nuclei was observed at 1 hr after incubation of the drug with cells. (B) The colocalization of doxorubicin released from cLABL-DOX-NP was observed at 1 hr but with a less extent compared to free drug. (C) The released doxorubicin from untargeted NP localized in the nuclei was observed at 3 hr. The white arrow indicates the colocalization.

A





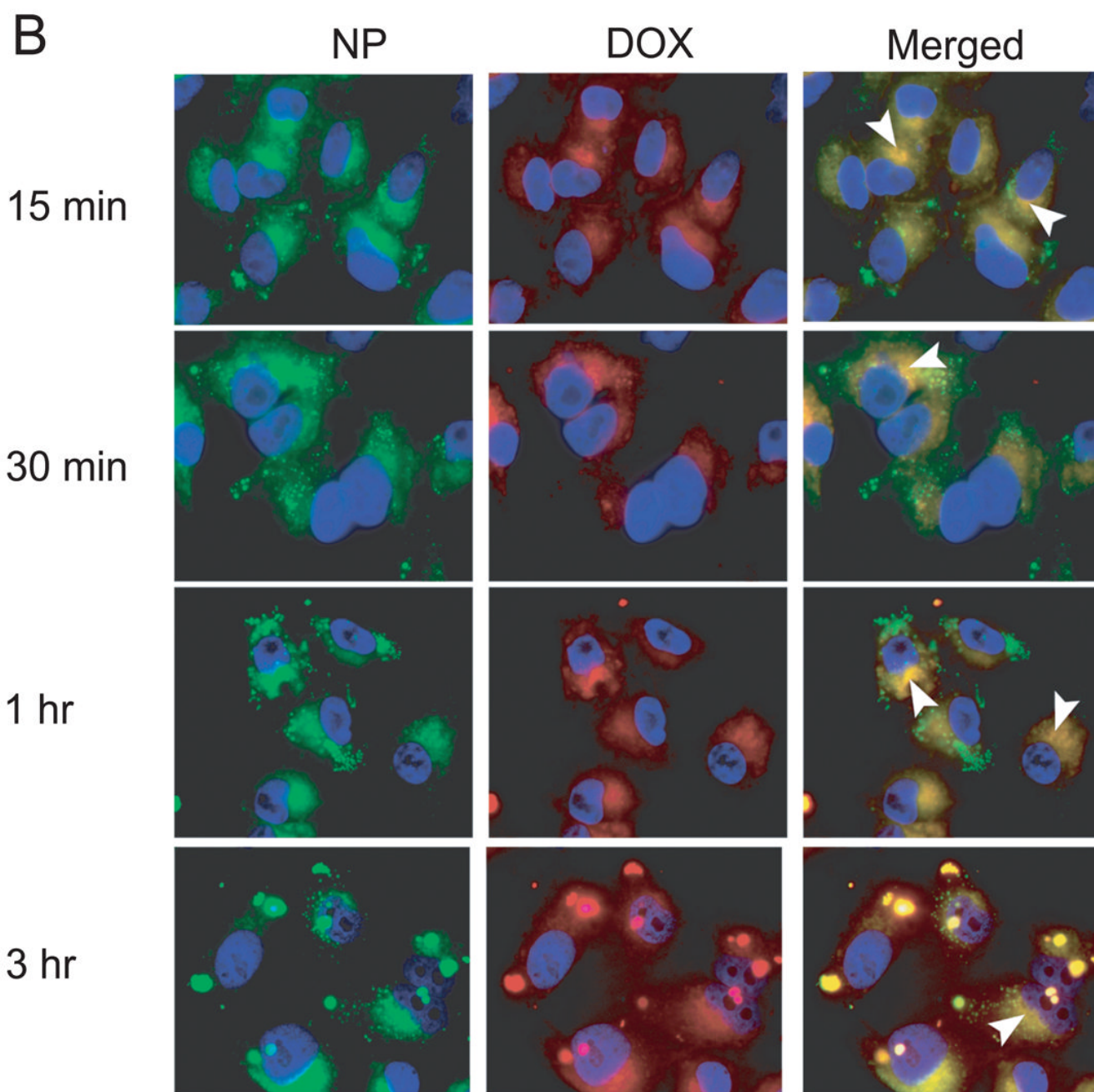


**Fig. 7.** (A), Colocalization of doxorubicin co-encapsulated with coumarin-6 in cLABL-DOX-NP (B) Colocalization of doxorubicin co-encapsulated with coumarin-6 in DOX-NP. The white arrow indicates the colocalization of coumarin-6 and doxorubicin.

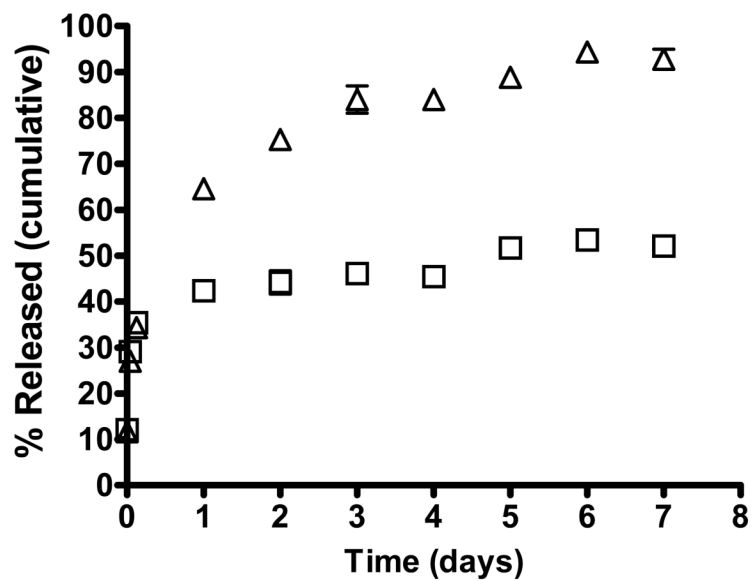


**Fig. 8.** The release of doxorubicin from cLABL-NP began with an initial burst of  $35.2 \pm 1.7\%$  and  $34.1 \pm 2.8\%$  at pH 4 (□) and pH 7.4(△), respectively, in the first three hours of the study. Data represented mean  $\pm$  S.D. (n=3).



Table 1

Nanoparticle properties prepared from PLGA 0.22 and 0.67 dl/g at specified formulation points

	Coumarin6-NP		eLABL-coumarin6-NP		DOX-NP		eLABL-DOX-NP	
	0.22	0.67	0.22	0.67	0.22	0.67	0.22	0.67
PLGA inherent - viscosity (dl/g)	224 ± 2.7	226 ± 4.5	243 ± 6.6	241 ± 0.8	264 ± 7.8	280 ± 15.4	303 ± 3.6	286 ± 10.3
Effective diameter (nm)	0.11 ± 0.03	0.10 ± 0.05	0.05 ± 0.01	0.07 ± 0.04	0.14 ± 0.07	0.19 ± 0.01	0.15 ± 0.01	0.19 ± 0.09
Zeta potential value (mV)	-47 ± 3.1	-45 ± 2.8	-49 ± 3.8	-59 ± 2.8	-29 ± 0.4	-38 ± 3.0	-43 ± 0.6	-45 ± 3.2

Values are representative of three determinations (mean ± S.D.)

**Table 2**

Encapsulation efficiency (%) of coumarin-6 and doxorubicin in nanoparticles

	Encapsulation efficiency (%)			
	Coumarin6-NP	cLABL-coumarin6-NP	DOX-NP	cLABL-DOX-NP
PLGA 0.22 dl/g	51 ± 1.2	33 ± 5.0	41 ± 4.8	19 ± 2.1
PLGA 0.67dl/g	60 ± 2.4	37 ± 1.3	51 ± 7.6	27 ± 5.4

Values are representative of three determinations (mean ± S.D.)

**Table 3**

Density of cLABEL on the surface of PLGA nanoparticles

	Size (nm)	Total surface area (m <sup>2</sup> /g of PLGA)	Surface cLABEL ( $\mu\text{mol}/\text{cm}^2$ ) <sup>a</sup>
PLGA 0.22 dl/g	243	18.4	55 $\pm$ 0.8
PLGA 0.67dl/g	241	18.6	51 $\pm$ 2.1

Values are representative of three determinations (mean  $\pm$  S.D.)